Human macrophages survive and adopt activated genotypes in living zebrafish.

Colin D Paul[1#], Alexus Devine[1#], Kevin Bishop[2], Qing Xu[3], Kathryn M Daly[1], Chaunte Lewis[1], Daniel S Green[4], Jack R Staunton[1], Swati Choksi[3], Zheng-Gang Liu[3], Raman Sood[2], and Kandice Tanner[1*]

[1] Laboratory of Cell Biology, Center for Cancer Research, National Cancer Institute, National Institutes of Health

[2] Zebrafish Core, National Human Genomic Research Institute, National Institutes of Health

[3]Laboratory of Immune Cell Biology, Center for Cancer Research, National Cancer Institute, National Institutes of Health

[4]Women's Malignancy Branch, Center for Cancer Research, National Cancer Institute, National Institutes of Health

[#] co-first authors

[*] To whom correspondence should be addressed: Kandice Tanner Ph.D., 37 Convent Dr., Bethesda, MD 20852. Email: kandice.tanner@nih.gov

Abstract

The inflammatory response, modulated both by tissue resident macrophages and recruited monocytes from peripheral blood, plays a critical role in human diseases such as cancer and neurodegenerative disorders. Here we sought a model to interrogate human immune behavior *in vivo*. We determined that primary human monocytes and macrophages survive in zebrafish for up to two weeks. Flow cytometry revealed that human monocytes cultured at the physiological temperature of the zebrafish survive and differentiate, comparable to cohorts cultured at human physiological temperature. Human cells migrated within multiple tissues at speeds comparable to zebrafish macrophages. Analysis of gene expression of *in vivo* educated human macrophages confirmed expression of activated macrophage phenotypes. Here, human cells adopted phenotypes relevant to cancer progression, suggesting that we can define the real time immune modulation of human tumor cells during the establishment of a metastatic lesion in zebrafish.

Keywords

Zebrafish, immune cells, live imaging, flow cytometry, human xenograft, cell migration, brain microenvironment, M1 and M2 phenotype, gene expression

Introduction

Macrophages represent a mature population of terminally differentiated cells of myeloid-lineage found in all tissues(1, 2). They are often categorized by distinct functional properties, cell surface markers, and the cytokine profile of the microenvironment. Highly plastic, macrophages adopt diverse phenotypic and functional states to regulate tissue homeostasis, tissue patterning, branching morphogenesis, wound repair and immunity(2). They respond to environmental cues within tissues such as damaged cells, activated lymphocytes, or microbial products to differentiate into distinct functional phenotypes(3). However, macrophages may adopt functions that aid and promote disease due to environmental cues that arise as a result of abnormal physiological states such as obesity, fibrosis, brain neurodegenerative disorders and cancer(1, 4-7). In particular, one of the "hallmarks" of cancer and predictors of aggressive metastatic disease is the chronic presence of activated myeloid cells, such as tumor associated macrophages (TAMs), within primary tumors(8-10). Probing the role of the inflammatory response in the earliest stages of malignant transformation remains technically and ethically difficult in human subjects. Nevertheless, the broad importance of immune cell biology necessitates appropriate models to adequately study implications in human disease.

A number of efforts have been made to "humanize" animal model systems to study human homeostasis and disease *in vivo*, especially in the context of blood cancers(11-17). However, the role of hematopoietic stem cells (HSCs) and their derivative lineages, such as myeloid cells, have also been identified as regulators of tumor progression for solid cancers(4, 8). There are several classes of macrophages that may be found around tumors(2, 10, 18). One class of macrophages includes the classical "M1" macrophage phenotype which is characterized by the production and secretion of elevated levels of pro-inflammatory cytokines, mediation of resistance to pathogens

63 with strong microbicidal properties, high production of reactive nitrogen and oxygen
64 intermediates, and evoking Th1 responses. In contrast, M2 macrophages are characterized by their
65 involvement in tissue remodeling, immune regulation, tumor promotion and efficient phagocytic
66 activity(2, 10). A second class of macrophages that mediate metastasis, metastasis-associated
67 macrophages (MAMs) is thought to drive therapeutic resistance and establish macrometastases at
68 distant sites(19, 20). However, probing the role of the inflammatory response on the etiology of
69 metastasis, namely when one or few cells have initiated the formation of a distant lesion in vivo,
70 is challenging. Of all the animal models of oncoimmunology, mice remain the standard model, as
71 one can interrogate human cells using immune-compromised strains and similarly examine
72 syngeneic cancer cell lines in the appropriate immune competent strain(11, 16, 21). However,
73 directly visualizing the colonization of multiple murine organs is expensive as it requires many
74 mice to achieve sufficiently powered statistics. Simply put, a model system that recapitulates
75 physiologically relevant aspects of metastatic disease in which cells can be observed at the single-
76 cell level would profoundly benefit metastatic cancer research(22).

77 Zebrafish larvae are optically transparent at larval stages and conducive for non-invasive
78 imaging *in vivo*. This, coupled with the fact that many processes involved in embryonic
79 development, cell biology, and genetics are conserved across vertebrates, makes zebrafish an
80 attractive model to study tumor-immune interactions during early stages of organ colonization(23,
81 24). In addition, organ architecture, composition and regulatory signaling networks for several
82 organs, including the brain, are well conserved in embryonic zebrafish(25, 26). As early as the first
83 few days after fertilization, key components of the Central Nervous System (CNS) such as
84 neurons, astrocytes, and microglia, as well as specialized structures such as the blood-brain barrier
85 and choroid plexus, have been identified in larval zebrafish. The innate immune system, comprised

primarily of neutrophils, tissue specific macrophages and peripheral derived monocytes/macrophages, is also conserved at this early developmental stage (15, 25, 26). Hence, the embryonic zebrafish offers a system in which cell dynamics can be observed while sharing key cellular and structural characteristics with the mammalian organs. This model can be used to delineate tissue resident vs. recruited circulating monocytes in the context of inflammation and tumor education for either primary brain tumors or in the case of early metastatic colonization. However, a key feature missing in studies of immune response in zebrafish is a careful demonstration that human immune cells can be introduced in this system with conserved survival and cell response.

Here, we introduced human monocytes/macrophages into the zebrafish directly into circulation and in an organ specific manner. We determined that both monocytes and macrophages (differentiated in culture) survive in innate immune competent zebrafish for up to two weeks post-injection despite the lower physiological temperature of the zebrafish (28.5°C). Similar results were obtained *in vitro*, where flow cytometry analysis revealed that human monocytes cultured at the physiological temperature of the zebrafish survive, differentiate, and show surface markers associated with mature macrophages in response to cytokines comparably to cohorts cultured at human physiological temperature (37°C). We also determined that human cells are transformed by zebrafish astrocytes by employing transgenic fish where fluorescently tagged astrocytes can be visualized *in vitro* and *in vivo*. Gene expression comparisons of *in vivo* educated human macrophages to *in vitro* cytokine-treated human macrophages revealed gene expression associated with activation. In summary, these results characterized the function of human immune cells in the *in vivo* environment and physiological temperature of *Danio rerio*. Thus, this model system allows for examination of the contribution of specific immune cells within specialized organ

109 microenvironments.

110 **Results**

111 Zebrafish are reared at the lower temperature of 28.5^{o}C compared to 37^{o}C, the
112 physiological temperature of mammals(27). Zebrafish also have an innate and adaptive immune
113 response beginning from two and nine days post fertilization, respectively). We thus asked if
114 human immune cells can survive at the physiological temperature of zebrafish in the presence of
115 the innate and immature adaptive immunity in an organ specific way. Human primary monocytes
116 that were differentiated into macrophages in culture were injected into the hindbrain of the
117 zebrafish. Longitudinal imaging of the same fish one day and 7 days post injection (3dpf and 9dpf,
118 respectively) revealed that human macrophages survive for at least one week after injection and
119 can be found dispersed in the brain **(Figure 1A).** Similar examination of human macrophages
120 injected into fish where the host microglia are fluorescently tagged revealed survival and
121 distribution within the brain **(Supplementary Figure 1A).** We next examined the survival of an
122 immortalized human monocyte cell line under the same conditions. Similar survival and
123 morphologies were observed within the brain (**Supplemental Figure 1B)**. Examination of fish
124 two weeks post injection revealed that a few human macrophages can persist *in vivo* **(Figure 1B,**
125 **Supplemental Figure 1C).** As immune cells are involved in tissue remodeling and surveillance,
126 we next asked if the introduced monocytes show comparable motilities. We quantified the host
127 immune cells movement by tracking neutrophils and macrophages in addition to introduced
128 immune cell within the brain at 3 dpf. We determined that neutrophils move with an average speed
129 of 7 microns/minute, which was significantly greater than that of either the zebrafish brain resident
130 macrophages and the introduced monocytes. There was no significant difference between the

slower monocytes/zebrafish macrophages, where an average speed of 0.5-1 microns/minutes was observed **(Supplemental Figure 2).**

Immune cells are able to move from circulation to different tissues, therefore we asked if human cells would adopt similar phenotypes and survive in zebrafish. Human macrophages injected directly to the zebrafish circulation were found throughout the entire fish as early as ~3hrs. post injection and 1 day post injection **(Supplemental Movie 1, Figure 2A).** They were observed to be motile and moved within intersegmental vessels and within different tissues **(Supplemental Movie 1).** Imaging of fish at one day and 7 days post injection (3dpf and 9dpf respectively) revealed that human macrophages survive for at least one week after injection into the circulation and can be found to be dispersed in multiple tissues, including the gills, intersegmental vessels and caudal tissue (data not shown) **(Figure 2B).**

Macrophages represent a class of terminally differentiated monocytes, and we reasoned that survival may differ as a function of differentiation status when cultured at the physiological temperature of zebrafish. Thus, we directly compared survival of human monocytes cultured at the two different temperatures for a period of 7 days. A sub set of human monocytes were injected into the hind brain of the zebrafish. We imaged larva over the course of 3 days post injection at 24 hour intervals **(Figure 3A).** We determined that ~40% of monocytes from de-identified human donors survived at the zebrafish physiological temperatures and were viable up to 7 days of *in vitro* culture in only culture medium. In contrast, these same cells cultured at mammalian physiological temperatures showed rapid cell death and viability, where ~50% of cells underwent apoptosis after 2 days of *in vitro* culture in culture medium and only 10% of cells were present 7 days after plating **(Figure 3B).** Similar quantitation of *in vivo* monocyte survival determined that ~40% of monocytes survive up to 3 days post injection. Analysis of fish imaged serially over the

course of 1 day intervals revealed that 25-50% of cells survived in multiple transgenic lines after 2 days post injection (2dpi) **(Figure 3C).** There was no regional preference for survival as cells were observed throughout the fore, mid and hind brain of each animal **(Supplemental Figure 3)**.

We then investigated whether these human cells cultured at zebrafish physiological temperature are capable of differentiating into functional macrophages. Human monocytes differentiate into macrophages in response to *in vitro* addition of human macrophage colony stimulating factor (H-MCSF)(28). We observed that monocytes cultured in the presence of H-MCSF at the lower temperature were not adherent and remained spherical in suspension. In comparison, cells that were cultured at the higher temperature adopted the classical morphology of adherent elongated cells following treatment of H-MCSF for five days **(Figure 4A).** Immune cells respond to cytokines secreted by other cell types. To determine if monocytes/macrophages respond to zebrafish stroma, we co-cultured these immune cells with zebrafish astrocytes using transwell assays. Quantitation of cells that migrated in transwell assays revealed that a greater fraction of cells migrated in response to zebrafish astrocytes for each culture condition than under control conditions **(Figure 4B).** We determined that monocytes cultured in the presence or absence of differentiation media showed an increased survival at the zebrafish physiological temperatures, where ~40% of cells without H-MCSF, and ~70% of cells with H-MCSF, were viable up to 5 days of *in vitro* culture. In contrast, these same cells cultured at mammalian physiological temperatures showed reduced viability when cultured with or without differentiation media **(Figure 4C).** Macrophages derived from monocyte precursors adopt specific phenotypes depending on cues from the local tissue environment. We next analyzed cell surface markers using flow cytometry to monitor macrophage maturation. Cells that were cultured with M-CSF at both temperatures showed increased expression for the surface marker CD86 compared to cells that

were cultured in control media **(Figure 4D)(29).** This surface protein is an indicator of macrophage maturation. We also observed that monocytes differentiated at lower temperature were motile *in vivo*. Moreover, these macrophages showed similar motility to macrophages that were differentiated at the higher temperature **(Supplemental Movies 1 and 2).**

Monocytes that are subjected to M-CSF will differentiate into macrophage populations marked by expression of CD86 and CD206(30, 31). We thus asked if monocytes differentiated at the lower temperature will also show functional plasticity. Surface marker expression for differentiated human macrophages is observed after 5, 8 and 11 days of exposure for both physiological temperatures. However, when cells are cultured at the lower temperature there is a temporal delay in the expression of CD86 and CD206, compared to cells cultured at the higher temperature **(Figure 5).**

Neutrophils are also conserved in the axis of innate immunity in zebrafish(23). Neutrophils are the first line of defense and produce a sustained inflammatory response following introduction of foreign entities. In the brain, the resident macrophages are the microglia(26). To determine if there was a differential zebrafish neutrophil or microglia response, differentiated human macrophages cultured at each temperature were injected into the hindbrain of 2dpf zebrafish where either host neutrophils/ macrophages and vasculature were fluorescently labeled. Serial imaging of the same fish one day and 7 days post injection (3dpf and 9dpf respectively), revealed that macrophages differentiated at each temperature survive for at least one week after injection and can be found dispersed in the fish brain as observed in previous transgenic lines. We determined that similar numbers survived in either line **(Supplemental Figure 4A),** with survival rates comparable to those observed in previous experiments. However, no swarming of neutrophils was observed in the vicinity of the human monocytes at 1 day or 7 days post injection. Micrographs

show that a few neutrophils are in close proximity to human macrophages. They adopt elongated and spherical phenotypes and are seen along blood vessels and in the brain parenchyma **(Figure 6, Supplemental Figure 4B-C).** We observed some co-localization between the host and human macrophages as determined by overlapping in the micrographs of the fish imaged 1 day post injection. However, very little overlap is observed one week post injection.

Macrophages can polarize into different phenotypes in response to cues from the local tissue microenvironment(29). Thus, we compared gene expression of macrophages exposed to known cytokines *in vitro* at the two temperatures. We determined that similar expression of TNF-α, CD163 and VEGF for human macrophages cultured *in vitro* in the presence of recombinant EGF and TNF-α for 24 hours at both physiological temperatures. However, there was a reduced expression of CCL18 for cells cultured at physiological temperature of zebrafish than at physiological temperature of humans **(Figure 7A).** We then compared gene expression of human cells that were injected in the zebrafish brain for 24 hours and revealed similar expression TNF-α and CD163 for human macrophages cultured *in vitro* at both physiological temperatures. However, there was a reduced expression of VEGF and CCL18 for cells cultured at physiological temperature of zebrafish compared to physiological temperature of humans **(Figure 7B).**

Discussion

Here, we humanized the zebrafish microenvironment by introducing human monocytes/macrophages. We first determined that human monocytes differentiate into functional macrophages at the physiological temperature of zebrafish. We showed that these human monocytes are able to survive for at least two-weeks post injection *in vivo* in immune competent fish. Specifically, in transgenic zebrafish where fluorophores coupled to promoters of either myeloid-specific peroxidase (*mpx)*, a homologue of myeloperoxidase, or macrophage expressed

gene 1 (*mpeg1*), allow specificity in distinguishing neutrophils from macrophages despite their common lineage. We used this distinction in lineage to analyze the survival and response of human immune cells introduced to embryonic zebrafish, demonstrating that human monocytes and macrophages injected into the zebrafish hindbrain or circulation survive and are functional for up to two weeks post-injection.

Transplantation of human hematopoietic stem cells (HSCs) and hematopoietic cancers have been successfully performed in fetal sheep, immunocompromised mice and zebrafish(10, 11, 16, 17, 24). In these animal models, the HSCs grafted successfully to the appropriate *in vivo* niche, bone marrow in mammals and kidney in the zebrafish, with varying lengths of survival *in vivo*. Moreover, the HSCs retained the ability to differentiate into multiple blood lineages, allowing the study of normal tissue homeostasis. This has greatly assisted in delineating what goes awry during transformation to cancers of the blood. Tissue grafting becomes more complicated in the case of cross species transplantation due to the mismatch in immune compatibility (11, 32). One solution involves sub-lethal irradiation of immune competent animals allowing for a temporal window whereby the donor components can be introduced (11, 32). However, there may be adverse and off-target effects due to the depletion of the recipient immune response. The zebrafish innate immune system comprised primarily of neutrophils and macrophages shows excellent conservation with mammals (15, 25). Here, we show that human monocytes/macrophages can survive *in vivo* in the larval zebrafish in the presence of innate immunity and immature adaptive immunity (**Figures 1 and 2, Supplemental Figures 1 and 2**). Interestingly, the introduced macrophages migrate through multiple tissues mimicking tissue surveillance, a key aspect of macrophage function **(Supplemental Movies 1 and 2).** Furthermore, they co-exist seemingly unmolested by host neutrophils and macrophages **(Figure 6, Supplementary Figure 4).** Thus,

246 there is sufficient conservation in signaling proteins that regulate immune survival. This suggests
247 that this model organism can provide a comparable study of metastases in the same manner as
248 observed in mice between host tissues of fish and human tumor cells.

249 In adult mammals, innate immune cells, monocytes and macrophages share a common
250 myeloid progenitor in the bone marrow (2, 10, 11, 33, 34). These cells differ greatly in their
251 lifespan, where peripheral blood derived monocytes (PBDM) survive just few days before
252 undergoing apoptosis. In contrast, differentiated monocytes such as macrophages may have a
253 lifespan of months. While these immune subsets are conserved in zebrafish innate immunity, the
254 major difference is that they exist at different physiological temperatures. This study showed that
255 human monocytes also survive on the order of days at the physiological temperature of zebrafish
256 and surprisingly, with a greater survival than a cohort cultured at the physiological temperature of
257 human *in vitro* and *in vivo* **(Figure 3).** Monocytes respond to different chemokines following a
258 strictly regulated schedule (2, 10, 11, 33, 34). Following dissemination from the bone marrow,
259 circulating monocytes are CCR2 negative. One example is that they become CCR2 positive
260 roughly 1- 2 days post release and successive tissue extravasation. Functional analysis revealed
261 that human monocytes differentiate into M0 macrophages as dictated by high CD86 and CD206
262 positive expressions at both temperatures in a similar time frame. However, monocytes cultured
263 at the lower temperature differentiate into mature macrophages with a temporal delay compared
264 to monocytes culture at human temperatures. In addition, the difference in morphology where
265 cells remained in suspension and did not adherent indicate that there are subtle differences due to
266 the mismatch of culture temperature. One reason could be reduced metabolism at the lower
267 temperature, or that the human cells follow the differentiation steps that zebrafish
268 monocytes/macrophages adopt. Nevertheless, the functional status is achieved **(Figures 4 and 5).**

Within a growing tumor, resident and recruited monocytes receive chemical cues from tumor-secreted chemokines and physical cues from the microenvironment such as hypoxia(35). Consequently, they become tumor-educated and adopt phenotypes that help drive tumor growth through promotion of neoangiogenesis, aberrant tissue remodeling, and development of immunosuppressive microenvironments(2, 4, 8). These tumor-associated macrophages (TAMs) are abundantly found within or adjacent to primary tumors in several types of human cancer. TAMs are regulated in part by colony stimulating factor (CSF)-1, mediated by the CSF-1 receptor (CSF1R), which drives macrophage maturation, tissue recruitment, and activation (36). Activated macrophages in turn release epidermal growth factor (EGF). At the primary tumor, this signaling pathway leads breast cancer cells and macrophages to form complexes that promote intravasation into the bloodstream (21, 37). There are several classes of macrophages that may be found around tumors. M1-type macrophages are thought to antitumorigenic and are characterized by high CD80, MHC-II, and PDL1 expression and low CD163 and CSF1R expression. In contrast, macrophages with high expression of CD68, CD163, CD206, and CSF1R are tumorigenic M2-type macrophages(20, 38) (18). Macrophages have been implicated in the clearance of circulating tumor cells during early metastatic dissemination (39, 40). Importantly, another class of macrophages, termed metastasis-associated macrophages (MAMs), may mediate metastasis, though the origins and recruitment of such macrophages are unclear(19, 20, 41). Here, we determined that in response to recombinant cytokines and brain-conditioning *in vivo*, human macrophages adopt gene expression that forms part of the identification of M1 and M2 phenotypes as measured by TNF-A, CD163 and VEG-F expression **(Figure 7).** M2 macrophages have been classified into subdivisions, a, b and c(42, 43). The M2a subtype can also be defined as alternative activated macrophages, the M2b as type 2 macrophages, and the M2c as deactivated macrophages.

The deactivated terminology refers to the *in vitro* ability of macrophages to adopt M2 activation following M1 activation, thus deactivating the M1-like gene transcription. Interestingly, CCL18 is differentially expressed as a function of culture conditions *in vivo* an *in vitro* **(Figure 7).** CCL18 production is associated with the M2c for human monocytes and macrophages(43, 44). These data suggest that human monocytes differentiated at the lower temperature may not show the plasticity to switch between phenotypes compared to the macrophages differentiated at the human temperature.

Brain metastasis remains a challenge in clinical settings as patient survival is still measured in weeks or months (45). Emerging data indicate that immune-mediated signaling plays an important role in the establishment of brain metastasis (46). However, what is less understood is the role of tissue specific microenvironment of the immune cells at early stages of colonization restricted to lesions well below the current methods of detection. In a spontaneous mouse model of melanoma, not only were disseminated tumor cells detected before clinically detected primary tumors, it was determined that metastatic growth at distal organs was regulated by a tissue specific immune response (47). Recently, in studies of mouse models of brain malignancies and confirmed in patient data, that in addition to tissue resident macrophages microglia, an abundance of bone marrow derived monocytes (BDMs) can be found even in an immune privileged organ such as the brain (48). Furthermore, they uncovered that the resultant tumor associated populations were distinct based on the macrophage ontogeny within the brain. Here, we determined that human macrophages survive and become activated in the zebrafish brain environment. This model allows for examination of the contribution of immune signaling in a tissue specific manner. These findings open up the possibility of studying early metastatic events of human cancers in fish. More

314 importantly, it allows us to add the complexity of human tumor-human immune interactions whilst
315 maintaining single cell resolution.

316 **Methods**

317 **Cells and Reagents**

318 **Animal studies**

319 Animal studies were conducted under protocols approved by the National Cancer Institute, and the
320 National Institutes of Health Animal Care and Use Committee. In our experiments, we employed
321 several transgenic lines, i.e. Tg(mpeg1:GFP), Tg(gfap:GFP) and Tg(mpx:GFP),
322 Tg(kdrl:GFP)la116 and Tg(kdrl:mCherry-CAAX) ^{y171}, kindly provided by Brant Weinstein
323 (NICHD, Bethesda, MD), and the Casper strain, a kind gift from David Langenau (Harvard
324 MGH)(49-51). Dual labeled vasculature and immune/astrocyte cells were generated by crossing
325 Tg(kdrl:mCherry-CAAX) ^{y171} and GFAP:GFP , Mpeg:GFP or Mpx:GFP. Progeny were screened
326 using fluorescence microscopy to identify those that expressed fluorescent markers for vasculature
327 and astrocytes, macrophages and neutrophils respectively. From this pool, founders were selected
328 for continuation of the line. Zebrafish were maintained at 28.5°C on a 14-hour light/10-hour dark
329 cycle according to standard procedures. Embryos obtained from natural spawning, raised at 28.5°C
330 and maintained in egg water containing 0.6 g sea salt per liter of DI water were checked for normal
331 development. At day 5 regular feeding commenced.

332 **Primary human monocytes- Maintenance and Macrophage differentiation protocol and**
333 **functionality assays**

334 Elutriated monocytes from 8 de-identified healthy human donors were acquired from the NIH,
335 Department of Transfusion Medicine (DTM) (according to NIH protocol 99CC0168). Donors
336 within the age group of 21-50 of either sex were selected for all experiments. Primary monocytes

were cultured in DMEM high glucose, 10% fetal bovine serum and 1% penicillin/streptomycin. Cells were either cultured at physiological temperature of humans (37°C) or at physiological temperature of zebrafish (28.5°C). These cells were cultured at a concentration of 1.1 $\times 10^6$ cells /cm^2 for minimum of five days to facilitate macrophage differentiation in the presence of recombinant human M-CSF (25 ng/ml). Media was replenished every 3 days. Samples were prepared for a minimum of three technical replicates for each donor sample. For comparison, a human monocyte cell line, U937 was cultured in suspension in RPMI media (ThermoFisher Scientific, Waltham, MA) supplemented with final volume of 10 % (v/v) Fetal Bovine Serum (FBS), Penicillin (100 U/mL) and Streptomycin (100 µg/mL). Cells were cultured at 37°C with 5% CO_2 and relative humidity maintained at 95%. Media was refreshed every 2- 3 days.

Primary monocytes that had been cultured in the presence of human M-CSF for eight days were cultured at each temperature (28.5 vs. 37°C). Cells cultured at each temperature were then cultured for an additional 24hrs with a vehicle control and in the presence of either recombinant EGF at a concentration of 10ng/ml or TNF-α at a concentration of 20ng/ml. In addition, 2-5nL of a sub set of the originally differentiated cells were then injected into 2dpf fli:GFP embryos at a concentration of 1×10^7 cells/mL for comparison. After 24hrs, RNA was extracted for the in vivo educated macrophages and the cells cultured in the presence of the cytokines. Similarly, RNA was extracted from pooled samples of 50 3dpf embryos for each temperature (28.5 vs. 37°C) and age matched uninjected embryos.

Quantification of *in vitro* monocyte survival at different physiological temperatures

For cell survival, human monocytes from 5 donors were seeded at a concentration of 1.1 $\times 10^6$ cells /cm^2 and cultured at either 28.5°C or 37°C in base media. Human monocytes were collected and centrifuged at 1000rpm for 5 minutes. Supernatant was removed and cells were resuspended in

1mL of sterile 1× PBS. Cells were collected at 2, 3, 5 and 7 days after plating and analyzed for cell number and viability using Nexcelom Bioscience Cell Counter. Technical triplicates were collected for each donor sample for each temperature and day to obtain an average fraction survival per donor. Data were then displayed using GraphPad Prism 7.0a to graph cell number and viability as a function of days and temperature. Two-way ANOVA was used to determine statistical significance. Bright field and epi-fluorescent images were obtained on a Zeiss Axiovert 200 with an AxioCam MRm, using AxioVision LE 4.8.2 software. Images were acquired using 10× air objective with numerical aperture, 0.25, where each individual image had lateral dimensions of 1388 × 1040 square pixels corresponding to 0.448 × 0.335 mm^2.

Quantification of *in vivo* monocyte survival

Image processing was performed via ImageJ. Spectral crosstalk was removed by subtracting contributions of the red channel from the far-red detection channel. Images were then median (radius of 3 pixels) and Gaussian (sigma of 2) filtered to minimize background noise. Binary masks of monocytes were generated using Huang and Otsu thresholding methods on corrected images. The volume occupied by monocytes was then calculated using ImageJ's built in 'analyze particles' function and the 3D shapes plugin. Number of monocytes was estimated by dividing the total volume of the binary monocyte mask by the expected average volume of a human monocyte (10 μm in diameter, volume of 104.7 μm^3). Loss of monocytes was calculated for each larva by subtracting final number of monocytes from the initial number of monocytes (24 hours post injection) then normalizing by the initial number of monocytes. Percent survival was reported as 1 minus loss of monocytes multiplied by one hundred.

As an example:**[100* (1- ((#24hpi - #48hpi) / #24hpi)]**

Data were then displayed using GraphPad Prism 7.0a to graph cell number and viability as a

383 function of days. All error bars are 95% confidence intervals where D'Agostino and Pearson
384 normality test was performed and Kruskal-Wallis test was performed to determine statistical
385 analysis.

386 **Flow cytometry to determine cell surface expression to determine phenotype**

387 Cells cultured in the absence and presence of human M-CSF were processed at minimum five days
388 after plating for flow cytometry. Cells that remained in suspension were collected whereas
389 adherent cells were detached with 2mM EDTA in PBS. For both conditions, the cell suspension
390 was centrifuged and the supernatant removed as previously described. The cell pellets were re-
391 suspended in ice-cold PBS with the following antibodies to assess surface expression for
392 determination of macrophage polarization. Cells were incubated on ice with CD86-PE (BD), or
393 CD206-APC (BD) antibodies for 1 hour and cells were washed twice before processing for flow
394 cytometry. For propidium iodide (11) staining, cells were washed and resuspended in HEPES
395 buffer containing PI. These markers for surface expression are indicative of M0 and M1
396 phenotypes and apoptosis, respectively. Samples were processed on a BD Calibur1 (BD
397 Biosciences) and analyzed with FlowJo software (Tree Star). PE- or APC-conjugated IgG stained
398 cells were used to indicate background fluorescence and to set quadrants before calculating the
399 percentage of positive cells.

400 **Fluorescence-activated cell sorting (FACS).**

401 Embryos at 2 days post fertilization (dpf) with labeled vasculature and astrocytes cells were
402 dechorionated in pronase solution (Roche Life Science #10165921001) as necessary (less than
403 5minutes). Embryos were then protease dissociated for FACS as previously described(52). Cell
404 sorting was performed on a FACSAria Fusion instrument (BD Biosciences, San Jose, CA) using
405 85µm nozzle at 45psi pressure. Cells were gated on forward and side light scatter and separated

406 based on GFP and/or mCherry-positive fluorescence signals defined with non-fluorescent negative
407 controls.

408 ***In vitro* migration assays.**

409 Astrocytes isolated from FACS were centrifuged at 1000 rpm for 5 minutes, resuspended and
410 counted. A 24-well plate was coated with 10 µg/ml laminin (Cytoskeleton Inc.) at room
411 temperature for 1 h prior to triplicate wash with PBS. Fluorescence-activated cell sorted astrocytes
412 were then added to the wells at 1 x 10^5 cells per mL (1 ml/well in 24-well plate). Zebrafish
413 astrocytes were maintained overnight in DMEM (Thermo Fisher)supplemented with 10% fetal
414 bovine serum, 1% penicillin-streptomycin and 1% L-glut at 28.5°C. The following day, cells were
415 prepared for transwell assay. Astrocytes were washed once with serum free RPMI medium. 700µl
416 of serum-free media was placed on top of astrocytes. A sterile transwell membrane with 8 µm
417 pores (Corning #3422) was inserted and 300µl of human macrophages were placed on top of
418 membrane at 5 x 10^4 cells per membrane. Transwells were incubated overnight at 33^{o}C. Three
419 membranes were run in parallel per condition (temperature and presence/absence of zebrafish
420 astrocytes). Transwells were fixed in 4% paraformaldehyde for 10 minutes at room temperature.
421 Membranes were washed twice in 1X PBS. They were permeablized using 0.1% triton-x 100 for
422 5 minutes at room temperature, followed by a second wash step and then processed for
423 immunofluorescence. Staining mixture consisted of Hoechst 33258 (10mg/mL, Thermo Fisher)
424 was used at 1µg/mL in 1% BSA-PBS along with Phalloidin 565 (Sigma) used at 20µl/mL of
425 Hoechst mixture. The membranes were imaged using Zeiss 780 LSM to acquire 5 x 5 tile scan
426 images of each membrane, using a 10× air objective of 0.3 NA where each individual image
427 comprised 2046 × 2046 square pixels corresponding to 1416 × 1416 square µm for a total Z
428 distance of 100 µm with 5 µm step size. Three randomly selected 500 x 500µm fields of view were

used for data analysis. We simultaneously excited our sample with the 405 nm from an argon ion laser with a power of < 3 % (total power 30 mW) and 546 nm from a solid-state laser (power of < 10 %). A secondary dichroic mirror, SDM 560, was employed in the emission pathway to delineate the red (band-pass filters 560–575 nm) and blue channels (480-495 nm) at a gain of 400 on the amplifier. The laser power for the 543 nm setting was set at < 3 % of the maximum power and the gain on the detectors was set to 450. The Hoechst-stained cell nuclei were counted. The lower Z represents the bottom of the membrane and higher Z represents the top of the membrane. Nuclei counted as through were on the bottom or in pores. Nuclei counted on top were used in total cell count. Data were displayed using GraphPad Prism 7.0a to graph cell migration with given attractants. Two-way ANOVA with Tukey's multiple comparisons post-test among all conditions was used to determine statistical significance.

Zebrafish injections

For all experiments, at 24 hours post fertilization (hpf), embryos were transferred to egg water supplemented with phenylthiourea (PTU, Sigma P5272), suspended at 7.5% w/v in DMSO, at 1 part in 4500 to inhibit melanin formation for increased optical transparency. Embryos were then returned to the incubator at 28.5°C and checked for normal development. Zebrafish embryos at 2 days post fertilization (2dpf) were anesthetized using 0.4% buffered tricaine. Human monocytes/macrophages were labeled with cell tracker (Green or Deep Red, Invitrogen) at a final concentration of 1 μM for 30 minutes. Cells were then centrifuged and the supernatant removed and pellet resuspended in PBS with a final cell concentration of 1×10^7 cells/mL before injection. 2-5 nL of labeled cells were injected into the hindbrain of the embryo. Fish were then reared at 28.5°C with 5% CO_2 and relative humidity maintained at 95% for two days. At 5 days post fertilization, some fish were then returned to system water and regular feeding at 28.5 °C for long-

term survival studies. For injection to the circulation, zebrafish were anesthetized in 0.4% buffered tricaine and oriented in a lateral orientation on an agarose bed. Cells were injected directly in the circulation via the posterior cardinal vein using a pulled micropipette. Fish were screened within 24 h of injection to check for successful introduction of cells to the circulatory system

Intravital microscopy

For live cell imaging, embryos were anesthetized using 0.4% buffered tricaine, then embedded in a lateral orientation in 1% low melting point agarose (NuSieve GTG agarose, Lonza), and allowed to polymerize in with cover glass (no. 1.5 thickness) as previously described (53). Egg water supplemented with tricaine was added to the agarose hydrogel for the entire time of data acquisition. Fish were imaged on Zeiss 710 or 780 laser scanning confocal microscopes. Initial overview experiments were taken at 20×, with 1 µm Z steps, as tile scans over the entire length and height of the fish. Images in the head and tail of the zebrafish were acquired at 10× magnification every 10 min for 14 h. Z stacks were acquired using a tiled approach and a 10× air objective of 0.3 NA where each individual image comprised 2046 × 2046 square pixels corresponding to 1416 × 1416 square µm for a total Z distance of 276 µm. One-photon, confocal, 2-dimensional images of 512 × 512 pixels (lateral dimensions) were acquired with a 1.4 NA 40 × oil-immersion objective. We simultaneously excited our sample with the 405 nm, 488 nm lines from an argon ion laser with a power of < 3 % (total power 30 mW) and 546 nm from a solid-state laser (power of < 10 %). A secondary dichroic mirror, SDM 560, was employed in the emission pathway to delineate the red (band-pass filters 560–575 nm) and green (band-pass filters 505–525 nm) and blue channels (480-495 nm) at a gain of 400 on the amplifier. The laser power for the 543 nm setting was set at < 3 % of the maximum power and the gain on the detectors was set to 450.

RNA isolation and Real-time PCR

Total RNA was extracted with Trizol according to the manufacturer's guidelines (Invitrogen). Any remaining DNA was removed with the DNA-free kit (Ambion) and was re-purified with the RNAeasy kit (Qiagen). Taqman real-time gene expression assays were run on an ABI StepOne Plus system according to manufacturer's protocol (Applied Biosystems). Gene expression was normalized to that of GAPDH or β-actin. All Taqman real-time primers used for gene-expression analysis were pre-designed and confirmed either from Integrated DNA Technologies: human TNFa (Hs.PT.45.14765639), VEGFA (Hs.PT.58.21234833), GAPDH (Hs.PT.39a.22214836) or from Life Technologies: human CD163 (Hs 00174705), CCL17 (Hs01128674).

Intravital cell tracking

Time-lapse microscopy images were exported to FIJI for analysis. To adjust for fish growth during imaging, images were first registered using the Correct 3D Drift plugin, with the vasculature of the fish used as a topographical reference. Cancer cells were then tracked in 3D using the TrackMate plugin for FIJI. Images were segmented in the cell fluorescence channel in each frame using a Laplacian of Gaussian (14) detector with a 15 µm estimated particle diameter. An initial threshold of 1.0 was set, and the sub-pixel localization and median filter options in TrackMate were activated. Segmentation was then further refined by manual adjustment of the threshold to minimize the non-macrophage particles selected. Segmented objects were linked from frame to frame with a Linear Assignment Problem (LAP) tracker with 30 µm maximum frame-to-frame linking distance. Tracks were visually inspected for completeness and accuracy over the entire acquisition period and were manually edited to ensure that point-to-point tracks were generated for the entire time that a cell was in the field of view.

Calculation of Cell Speed

Temporal and spatial information for each cell track was exported to MATLAB. For each cell, frame-to-frame speed was calculated by dividing the displacement of the cell by the time interval between frames. An average speed for that cell over the course of imaging was then calculated by averaging these frame-to-frame speeds. The ensemble of cell speeds in each location (head, tail, trunk) was compared in GraphPad Prism 7 using one-way ANOVA with Tukey's multiple comparisons post-test.

Author Contribution

K.T., Z.L, S.C, R.S., D.G. designed and discussed experiments, K.T., K.B., C.P., Q.A.D., C.L, A.W. performed experiments, K.T., C.P., A.D., K.D., Q.X., C.L, J.S, performed data analysis. K.T, C.P., S.C. wrote the main manuscript text. K.T., C.P, Q.X., K.D., J.S., prepared figures. All authors reviewed the manuscript.

Additional Information

The authors declare no competing financial interests.

Acknowledgements

This research was supported by the Intramural Research Program of the National Institutes of Health, the National Cancer Institute. We would like to thank Susan Garfield and Langston Lim, CCR Confocal Microscopy Core Facility, Laboratory of Cancer Biology and Genetics, NCI for use of the core microscopes. Cell sorting was performed by the NCI LGI Flow Cytometry Core supported by funds from the Center for Cancer Research, National Cancer Institute. We would like to thank Ashley Williams for assistance in preliminary monocyte differentiation experiments.

Figure Legend

Figure 1- Human macrophages survive *in vivo* for up to two weeks post injection following Brain injection

A) Micrographs of 3D projections showing distribution and survival of human primary macrophages (blue) injected into the hind brain of transgenic zebrafish embryos mpx:GFP (neutrophils-green)/flk:mCherry (vessels-red) at 2 days post fertilization (2dpf). Left panel 1 day post injection (1dpi) when embryo is 3dpf and right panel, same fish 7dpi when at 9dpf. Scale bar = 100 µm.

B) Micrographs show that cells can persist for up to 2 weeks after injection at 16dpf. Left panel: micrograph shows tiled image of the 16dpf zebrafish, white square highlights region of interest in the zebrafish brain. Scale bar = 500 µm. Right panel: micrograph of the inset where the white arrows indicate human cells. Scale bar = 100 µm.

Figure 2- Human macrophages survive *in vivo* for up to one week post injection following injection directly into the circulation of the zebrafish

A) Top panel: Schematic showing experimental set up where human macrophages were directly injected into the circulation of 2 days post-fertilization, 2dpf embryos. Middle panels: micrograph shows tiled image of the 3dpf zebrafish, 1 day post injection (1dpi) showing distribution and survival of human primary macrophages

(blue) injected into transgenic zebrafish embryos, fli:GFP (vessels-green). Bottom panels: Micrographs of 3D projections at higher magnification of insets highlighted in tiled images showing distribution and survival of human primary macrophages (blue).

B) Top panel: micrograph shows tiled image of the 9dpf zebrafish, 7 days post injection (7dpi) showing distribution and survival of human primary macrophages (blue) injected into transgenic zebrafish embryos, fli:GFP (vessels-green). Bottom panel: Micrographs of 3D projections at higher magnification of insets highlighted in tiled image showing distribution and survival of human primary macrophages (blue).

Figure 3- Primary human monocytes survive at physiological temperature of the zebrafish *in vitro* and *in vivo*.

A) Primary human monocytes (blue) were injected into the hind brain of transgenic zebrafish embryos, GFAP:GFP (astrocytes-green)-flk:mCherry (vessels-red) at 2dpf. Micrographs show representative images where fish was imaged serially over the course of 3 days post injection at interval of 24hrs.

B) Cells were either cultured at physiological temperature of humans (37°C) or at physiological temperature of zebrafish (28.5°C). Plot (mean±SD) of average survival calculated for primary human monocytes obtained from 4 donors where the numbers of cells that survived over the course of 7 days were normalized to the

561 original seeding density. Days in culture was a statistically significant factor in
562 survival by two-way ANOVA.
563 C) Plot (mean±SD) of average *in vivo* survival calculated for primary human
564 monocytes obtained from 50 larvae where the numbers of cells that survived over
565 the course of 3 days were normalized to the initial numbers measured one day post
566 injection. Statistical analysis where ** indicates a p value of $p<0.01$ and ****
567 indicates a p value of $p<0.0001$ by. Scatter plots show values for individual fish. Not
568 all fish survived to 5 days post injection.
569 **Figure 4- Flow cytometry determined that primary human monocytes can**
570 **survive and differentiate into macrophages at physiological temperature of the**
571 **zebrafish *in vitro***
572 Human primary monocytes were cultured at physiological temperature of zebrafish
573 (28.5°C) or at physiological temperature of humans (37°C) with or without
574 differentiation by cytokine human macrophage colony stimulating factor (H-MCSF)
575 for five days. A) Micrographs show the morphology of cells in the presence or
576 absence of cytokine. B) Graphs (mean±SD) showing fraction of migrated cells in
577 response or absence of isolated zebrafish astrocytes in a transwell assay. *, $p<0.05$
578 by Tukey's multiple comparisons post-test. C) Primary monocytes from 5 donors
579 were either cultured at physiological temperature of humans (37°C) or at
580 physiological temperature of zebrafish (28.5°C) with or without H-MCSF. Plot

(mean±SD) of average survival calculated for primary human monocytes/macrophages that survived over the course of 5 days were normalized to the original seeding density. Significantly more cells survived at 28.5°C vs. 37°C in the presence or absence of H-MCSF by two-way ANOVA. D) Flow cytometry where expression for CD86 was determined for each condition. Red curve indicates control where shift in blue curve indicates induced expression.

Figure 5- Flow cytometry determined primary human monocytes take a longer time to differentiate into macrophages at physiological temperature of the zebrafish *in vitro*

Human primary monocytes were cultured at physiological temperature of zebrafish (28.5°C,left panels) or at physiological temperature of humans (37°C, right panels) with cytokine human macrophage colony stimulating factor (H-MCSF) for five, eight and 11 days. A-B) Flow cytometry where expression for CD86 andCD206were determined for each condition. Red curve indicates control where shift in blue curve indicates induced expression.

Figure 6- Primary human macrophages can survive at physiological temperature of the zebrafish *in vivo* and do not cause a sustained inflammatory response.

Monocytes that had been cultured in the presence of human macrophage colony stimulating factor (H-MCSF) for five days A) at physiological temperature of

(28.5°C) and B) at physiological temperature of humans (37°C). Primary human macrophages (blue) were injected into the hind brain of transgenic zebrafish embryos, Mpeg:GFP (macrophages-green)/flk:mCherry (vessels-red) or Mpx:GFP (neutrophils-green)/flk:mCherry (vessels-red) at 2 days post fertilization (2dpf). Micrographs of 3D projections showing distribution and survival of human primary macrophages 1 day post injection (1dpi) when larvae are 3dpf and right panel, same fish at 7dpi when larvae are 9dpf.

Figure 7- Primary human macrophages show gene expression of activated phenotypes *in vivo* comparable to macrophages cultured *in vitro* at physiological temperatures of the zebrafish and human

A) Graphs show relative gene expression in specific markers for TNF−α and CD163, CCL18, VEGF for human macrophages cultured *in vitro* in the presence of recombinant EGF and TNF−α for 24 hours at physiological temperature of zebrafish (28.5°C) or at physiological temperature of humans (37°C).

B) Graphs show *in vivo* relative gene expression in specific markers for TNF−α and CD163, CCL18,VEGF for human macrophages after 24 hours injected into the brain of the zebrafish.

Supplemental Figure 1- Human immortalized monocytes and primary macrophages survive *in vivo* for one week

A) Micrographs of 3D projections showing distribution and survival of human primary macrophages (blue) injected into the hind brain of transgenic zebrafish embryos, Mpeg:GFP (zebrafish macrophages-green), at 3 days post fertilization (3dpf). Left panel shows 1 day post injection (1dpi) when larvae is 3dpf and right panel, same fish 7dpi when at 9dpf. Scale bar = 100 µm.

B) U937 human monocytes (blue) were injected into the hind brain of transgenic zebrafish embryos, GFAP:GFP (astrocytes-green)/flk:mCherry (vessels-red) at 2 days post fertilization (2dpf). Left panel shows 3D projection of injected cells on the day of injection, with detail shown in the inset. Right panel illustrates that these cells can survive over time, showing injected embryo one week after injection at 9 dpf.

C) Micrographs show that cells can persist for up to 2 weeks after injection into Mpx:GFP (neutrophils-green)/flk:mCherry (vessels- red) at 2 days post fertilization (2dpf). Left panel: micrograph shows tiled image of the 16dpf zebrafish, white square highlights region of interest in the zebrafish brain. Scale bar = 500 µm. Right panel: micrograph of the inset where the white arrow indicates the human cell in contact with the blood vessel in the mid-hind brain. Scale bar = 100 µm.

Supplemental Figure 2- Human immortalized monocytes show similar motilities to zebrafish immune cells *in vivo*

A) Plot (mean±SD) of average speeds calculated for brain resident zebrafish macrophages, neutrophils and human monocytes (U937) *in vivo*. Statistical analysis where **** indicates $p<0.0001$ by ordinary one-way ANOVA with Tukey's multiple comparisons post-test.

B) Micrographs show initial position of cells and final position of cells for up to 60 minutes where average speed of human monocytes was calculated from 3D images. Top panel- brain resident zebrafish macrophages, middle panel- brain resident zebrafish neutrophils and bottom panel- human monocytes injected into the hind brain.

Supplemental Figure 3- Primary human monocytes show similar survival in different strains *in vivo*.

A) Primary human monocytes (blue) were injected into the hind brain of transgenic zebrafish embryos, GFAP:GFP (astrocytes- green) at 2dpf. Micrographs show representative images where fish was imaged serially over the course of 2 days post injection (2dpi, 4dpf) at interval of 24hrs.

B) Primary human monocytes (blue) were injected into the hind brain of transgenic zebrafish embryos, Mpeg:GFP (zebrafish macrophages- green) at 2dpf. Micrographs show representative images where fish was imaged serially over the course of 2 days post injection (2dpi, 4dpf) at interval of 24hrs.

C) Top panel- Plot (mean±95% CI) of average *in vivo* survival calculated for primary human monocytes obtained from n=30 larvae for GFAP:GFP and n=7 larvae for Mpeg:GFP, where the numbers of cells that survived over the course of 2days were normalized to the initial numbers measured one day post injection. Bottom panel- Graph displays relative distribution of survival based on the initial number of cells.

Supplemental Figure 4- Primary human macrophages differentiated at physiological temperatures of the zebrafish or human show similar survival in different strains *in vivo*

Primary human macrophages (blue) were injected into the hind brain of transgenic zebrafish embryos, Mpeg:GFP (macrophages- green)/flk:mCherry (vessels-red) or Mpx:GFP (neutrophils-green)/flk:mCherry (vessels-red) at 2 days post fertilization (2dpf).

A) Plot (mean±SD) of average *in vivo* survival calculated for primary human macrophages differentiated at physiological temperatures of the zebrafish or human obtained from 3 larvae each, where the numbers of cells that survived over the course of 7 days were normalized to the initial numbers measured one day post injection. Differences in survival were not significant by two-way ANOVA with Tukey's multiple comparisons post-test.

Same as Figure 6 with no bright-field B-C

679 Monocytes that had been cultured in the presence of human macrophage colony
680 stimulating factor (H-MCSF) for five days **B**) at physiological temperature of
681 zebrafish (28.5°C) and **C**) at physiological temperature of humans (37°C). Primary
682 human macrophages (blue) were injected into the hind brain of transgenic zebrafish
683 embryos, Mpeg:GFP (macrophages-green)/flk:mCherry (vessels-red) or Mpx:GFP
684 (meutrophils-green)/flk:mCherry (vessels-red) at 2 days post fertilization (2dpf).
685 Micrographs of 3D projections showing distribution and survival of human primary
686 macrophages 1 day post injection (1dpi) when larvae are 3dpf and right panel, same
687 fish at 7dpi (9dpf).
688
689 **Supplemental Movie Legend**
690 **Supplemental Movie 1**- Monocytes that had been cultured in the presence of human
691 macrophage colony stimulating factor (H-MCSF) for eight days at physiological
692 temperature of zebrafish (28.5°C) were directly injected into the circulation of 2 days
693 post-fertilization (2dpf) embryos. Movie shows average intensity projection
694 from 3D time-lapse ~3 hours post-injection for 15hours at a frame rate
695 of 20 seconds/Zstack (33 planes, 2 µm z step) every 10 minutes.
696 **Supplemental Movie 2**- Monocytes that had been cultured in the presence of human
697 macrophage colony stimulating factor (H-MCSF) for eight days at physiological
698 temperature of human (37°C) were directly injected into the circulation of 2 days

699 post-fertilization (2dpf) embryos. Movie shows average intensity projection
700 from 3D time-lapse ~3 hours post-injection for 15hours at a frame rate
701 of 20 seconds/Zstack (33 planes, 2 µm z step) every 10 minutes.
702

References

1. Wynn TA, Chawla A, & Pollard JW (2013) Macrophage biology in development, homeostasis and disease. *Nature* 496(7446):445-455.
2. Pollard JW (2009) Trophic macrophages in development and disease. *Nat Rev Immunol* 9(4):259-270.
3. Murray PJ, *et al.* (2014) Macrophage activation and polarization: nomenclature and experimental guidelines. *Immunity* 41(1):14-20.
4. Coussens LM & Werb Z (2002) Inflammation and cancer. *Nature* 420(6917):860-867.
5. Kingwell K (2012) Neurodegenerative disease: Microglia in early disease stages. *Nat Rev Neurol* 8(9):475.
6. Perry VH, Nicoll JA, & Holmes C (2010) Microglia in neurodegenerative disease. *Nat Rev Neurol* 6(4):193-201.
7. Lumeng CN & Saltiel AR (2011) Inflammatory links between obesity and metabolic disease. *Journal of Clinical Investigation* 121(6):2111-2117.
8. DeNardo DG, Johansson M, & Coussens LM (2008) Immune cells as mediators of solid tumor metastasis. *Cancer Metast Rev* 27(1):11-18.
9. Hanahan D & Weinberg RA (2011) Hallmarks of cancer: the next generation. *Cell* 144(5):646-674.
10. Vesely MD, Kershaw MH, Schreiber RD, & Smyth MJ (2011) Natural innate and adaptive immunity to cancer. *Annu Rev Immunol* 29:235-271.
11. Zitvogel L, Pitt JM, Daillere R, Smyth MJ, & Kroemer G (2016) Mouse models in oncoimmunology. *Nat Rev Cancer* 16(12):759-773.
12. AlmeidaPorada G, Ascensao JL, & Zanjani ED (1996) The role of sheep stroma in human haemopoiesis in the human/sheep chimaeras. *Brit J Haematol* 93(4):795-802.
13. Langenau DM & Zon LI (2005) The zebrafish: A new model of T-cell and thymic development. *Nature Reviews Immunology* 5(4):307-317.
14. Morton JJ, *et al.* (2016) XactMice: humanizing mouse bone marrow enables microenvironment reconstitution in a patient-derived xenograft model of head and neck cancer. *Oncogene* 35(3):290-300.
15. Renshaw SA & Trede NS (2012) A model 450 million years in the making: zebrafish and vertebrate immunity. *Dis Model Mech* 5(1):38-47.
16. Theocharides AP, Rongvaux A, Fritsch K, Flavell RA, & Manz MG (2016) Humanized hemato-lymphoid system mice. *Haematologica* 101(1):5-19.
17. Zanjani ED, AlmeidaPorada G, & Flake AW (1996) The human/sheep xenograft model: A large animal model of human hematopoiesis. *Int J Hematol* 63(3):179-192.
18. Ruffell B, Affara NI, & Coussens LM (2012) Differential macrophage programming in the tumor microenvironment. *Trends Immunol* 33(3):119-126.
19. Joyce JA & Pollard JW (2009) Microenvironmental regulation of metastasis. *Nat Rev Cancer* 9(4):239-252.
20. Wang J, *et al.* (2015) Novel mechanism of macrophage-mediated metastasis revealed in a zebrafish model of tumor development. *Cancer Res* 75(2):306-315.
21. Wyckoff JB, *et al.* (2007) Direct visualization of macrophage-assisted tumor cell intravasation in mammary tumors. *Cancer Res* 67(6):2649-2656.

22. Tanner K & Gottesman MM (2015) Beyond 3D culture models of cancer. *Sci Transl Med* 7(283):283ps289.
23. Renshaw SA & Trede NS (2012) A model 450 million years in the making: zebrafish and vertebrate immunity. *Disease Models & Mechanisms* 5(1):38-47.
24. White R, Rose K, & Zon L (2013) Zebrafish cancer: the state of the art and the path forward. *Nat Rev Cancer* 13(9):624-636.
25. Meeker ND & Trede NS (2008) Immunology and zebrafish: spawning new models of human disease. *Dev Comp Immunol* 32(7):745-757.
26. Oosterhof N, Boddeke E, & van Ham TJ (2015) Immune cell dynamics in the CNS: Learning from the zebrafish. *Glia* 63(5):719-735.
27. Sanders GE (2012) Zebrafish housing, husbandry, health, and care: IACUC considerations. *ILAR J* 53(2):205-207.
28. Gordon S & Martinez FO (2010) Alternative activation of macrophages: mechanism and functions. *Immunity* 32(5):593-604.
29. Zhang Y, *et al.* (2013) ROS play a critical role in the differentiation of alternatively activated macrophages and the occurrence of tumor-associated macrophages. *Cell Res* 23(7):898-914.
30. Tarique AA, *et al.* (2015) Phenotypic, functional, and plasticity features of classical and alternatively activated human macrophages. *Am J Respir Cell Mol Biol* 53(5):676-688.
31. Weiss M, Blazek K, Byrne AJ, Perocheau DP, & Udalova IA (2013) IRF5 is a specific marker of inflammatory macrophages in vivo. *Mediators Inflamm* 2013:245804.
32. Macchiarini F, Manz MG, Palucka AK, & Shultz LD (2005) Humanized mice: are we there yet? *J Exp Med* 202(10):1307-1311.
33. Gordon S & Taylor PR (2005) Monocyte and macrophage heterogeneity. *Nat Rev Immunol* 5(12):953-964.
34. Montali RJ (1988) Comparative pathology of inflammation in the higher vertebrates (reptiles, birds and mammals). *J Comp Pathol* 99(1):1-26.
35. DeNardo DG & Coussens LM (2007) Inflammation and breast cancer. Balancing immune response: crosstalk between adaptive and innate immune cells during breast cancer progression. *Breast cancer research : BCR* 9(4):212.
36. Sullivan AR & Pixley FJ (2014) CSF-1R signaling in health and disease: a focus on the mammary gland. *J Mammary Gland Biol Neoplasia* 19(2):149-159.
37. Wyckoff J, *et al.* (2004) A paracrine loop between tumor cells and macrophages is required for tumor cell migration in mammary tumors. *Cancer Research* 64(19):7022-7029.
38. Ries CH, *et al.* (2014) Targeting tumor-associated macrophages with anti-CSF-1R antibody reveals a strategy for cancer therapy. *Cancer Cell* 25(6):846-859.
39. Gul N, *et al.* (2014) Macrophages eliminate circulating tumor cells after monoclonal antibody therapy. *J Clin Invest* 124(2):812-823.
40. Pucci F, *et al.* (2016) SCS macrophages suppress melanoma by restricting tumor-derived vesicle-B cell interactions. *Science* 352(6282):242-246.
41. Quail DF & Joyce JA (2013) Microenvironmental regulation of tumor progression and metastasis. *Nat Med* 19(11):1423-1437.
42. Roszer T (2015) Understanding the Mysterious M2 Macrophage through Activation Markers and Effector Mechanisms. *Mediat Inflamm*.

43. Mantovani A, *et al.* (2004) The chemokine system in diverse forms of macrophage activation and polarization. *Trends Immunol* 25(12):677-686.
44. Schraufstatter IU, Zhao M, Khaldoyanidi SK, & Discipio RG (2012) The chemokine CCL18 causes maturation of cultured monocytes to macrophages in the M2 spectrum. *Immunology* 135(4):287-298.
45. Steeg PS (2016) Targeting metastasis. *Nat Rev Cancer* 16(4):201-218.
46. Erez N & Coussens LM (2011) Leukocytes as paracrine regulators of metastasis and determinants of organ-specific colonization. *International journal of cancer. Journal international du cancer* 128(11):2536-2544.
47. Eyles J, *et al.* (2010) Tumor cells disseminate early, but immunosurveillance limits metastatic outgrowth, in a mouse model of melanoma. *J Clin Invest* 120(6):2030-2039.
48. Bowman RL, *et al.* (2016) Macrophage Ontogeny Underlies Differences in Tumor-Specific Education in Brain Malignancies. *Cell Rep* 17(9):2445-2459.
49. Renshaw SA, *et al.* (2006) A transgenic zebrafish model of neutrophilic inflammation. *Blood* 108(13):3976-3978.
50. Ellett F, Pase L, Hayman JW, Andrianopoulos A, & Lieschke GJ (2011) mpeg1 promoter transgenes direct macrophage-lineage expression in zebrafish. *Blood* 117(4):e49-56.
51. Bernardos RL & Raymond PA (2006) GFAP transgenic zebrafish. *Gene Expr Patterns* 6(8):1007-1013.
52. Manoli M & Driever W (2012) Fluorescence-activated cell sorting (FACS) of fluorescently tagged cells from zebrafish larvae for RNA isolation. *Cold Spring Harb Protoc* 2012(8).
53. Blehm BH, Devine A, Staunton JR, & Tanner K (2016) In vivo tissue has non-linear rheological behavior distinct from 3D biomimetic hydrogels, as determined by AMOTIV microscopy. *Biomaterials* 83:66-78.

Figure 1

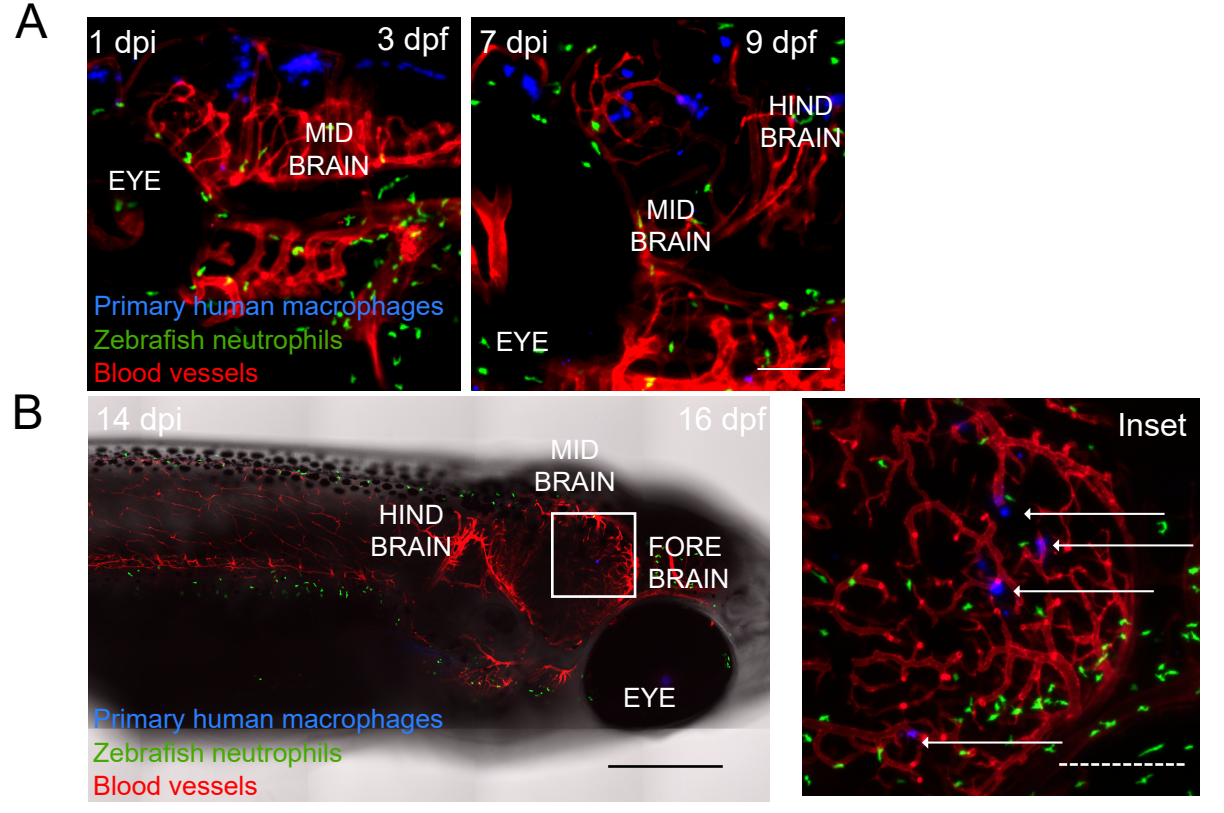
A
1 dpi
3 dpf
MID
BRAIN
EYE
Primary human macrophages
Zebrafish neutrophils
Blood vessels
7 dpi
9 dpf
HIND
BRAIN
MID
BRAIN
EYE
B
14 dpi
16 dpf
MID
BRAIN
HIND
BRAIN
FORE
BRAIN
EYE
Primary human macrophages
Zebrafish neutrophils
Blood vessels
Inset

Figure 2

A

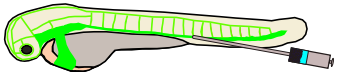

Blood vessels
Primary human macrophages

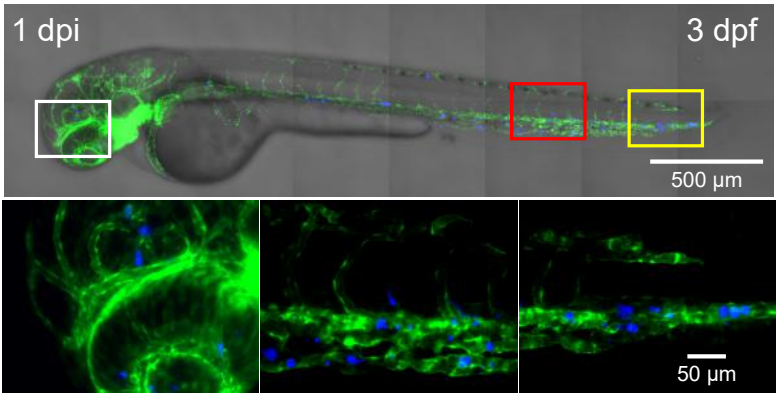

B

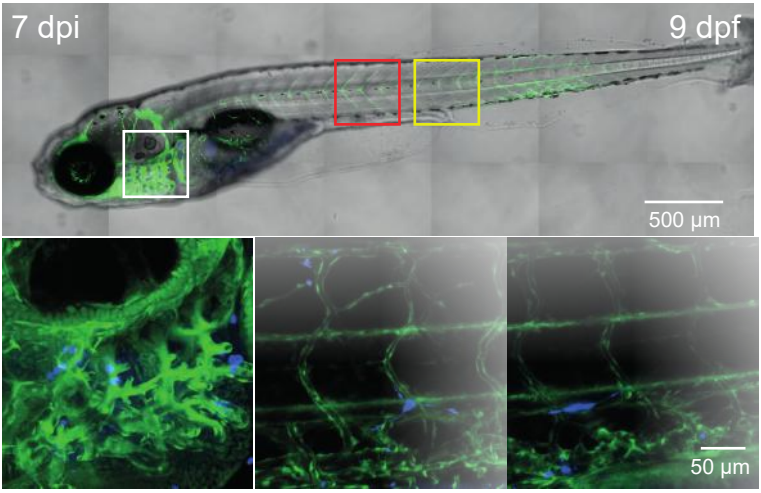

Blood vessels
Primary human macrophages

Figure 3

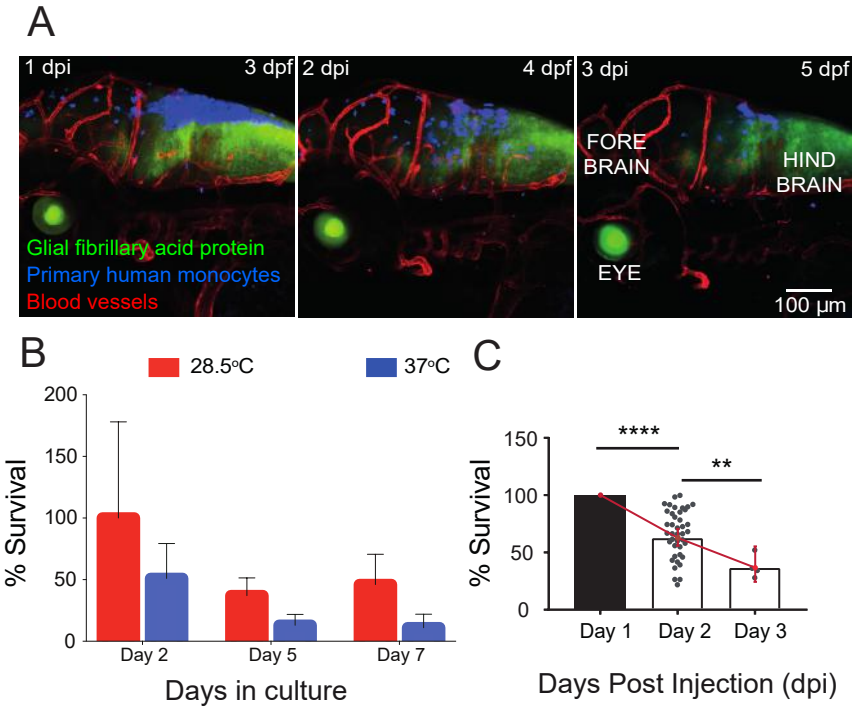

in vitro
Human Monocyte Cell Survival

in vivo
Human Monocyte Cell Survival

Figure 4

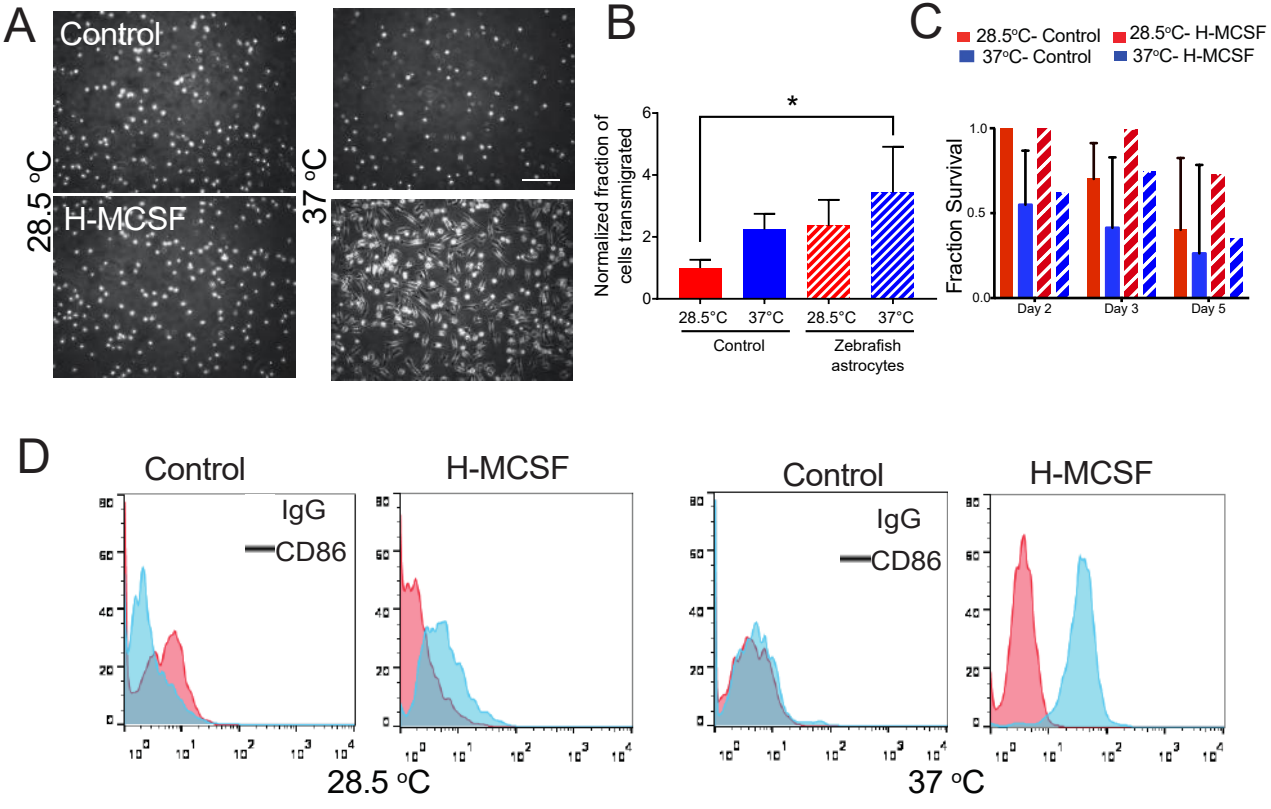
A
Control
H-MCSF
28.5 °C
37 °C
B
Normalized fraction of cells transmigrated
*
28.5°C
37°C
28.5°C
37°C
Control
Zebrafish astrocytes
C
28.5°C- Control
28.5°C- H-MCSF
37°C- Control
37°C- H-MCSF
Fraction Survival
Day 2
Day 3
Day 5
D
Control
H-MCSF
IgG
CD86
28.5 °C
37 °C

Figure 5

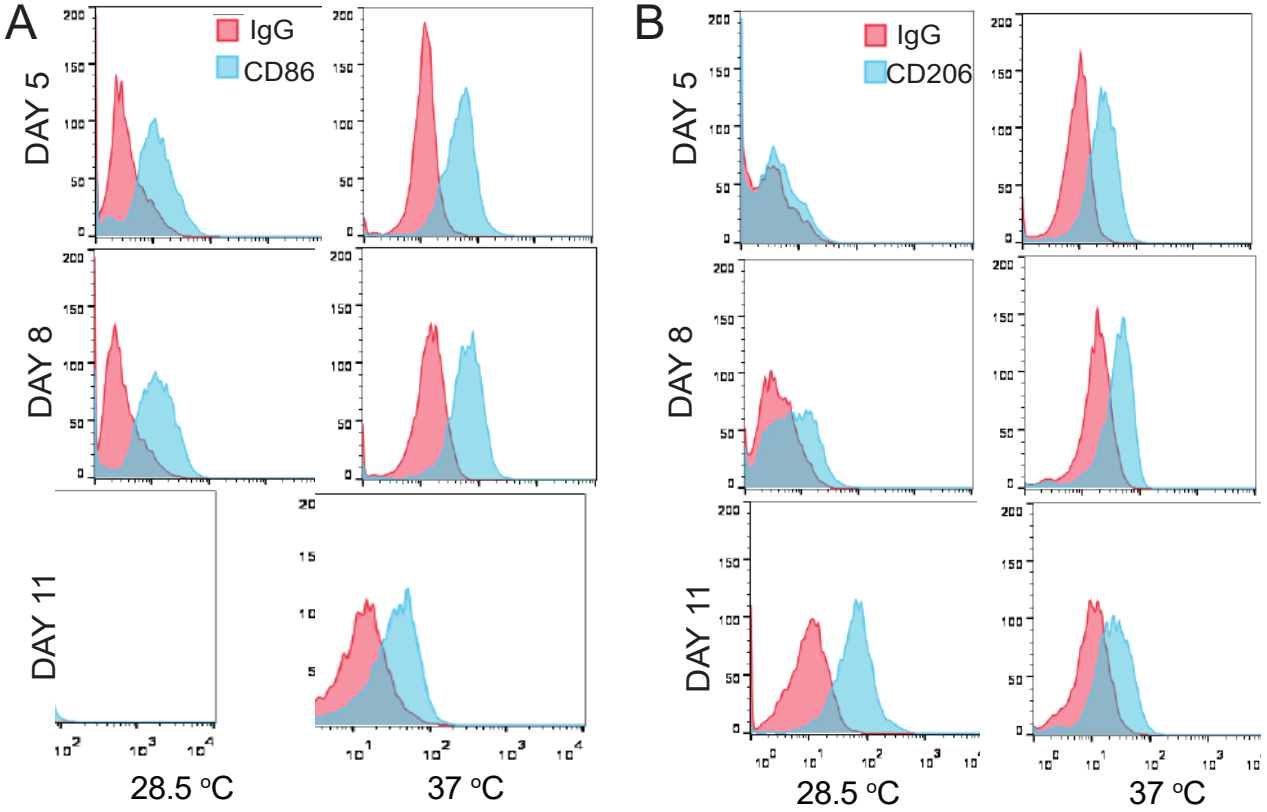
A
IgG
CD86
DAY 5
DAY 8
DAY 11
28.5 °C
37 °C
B
IgG
CD206
DAY 5
DAY 8
DAY 11
28.5 °C
37 °C

Figure 6

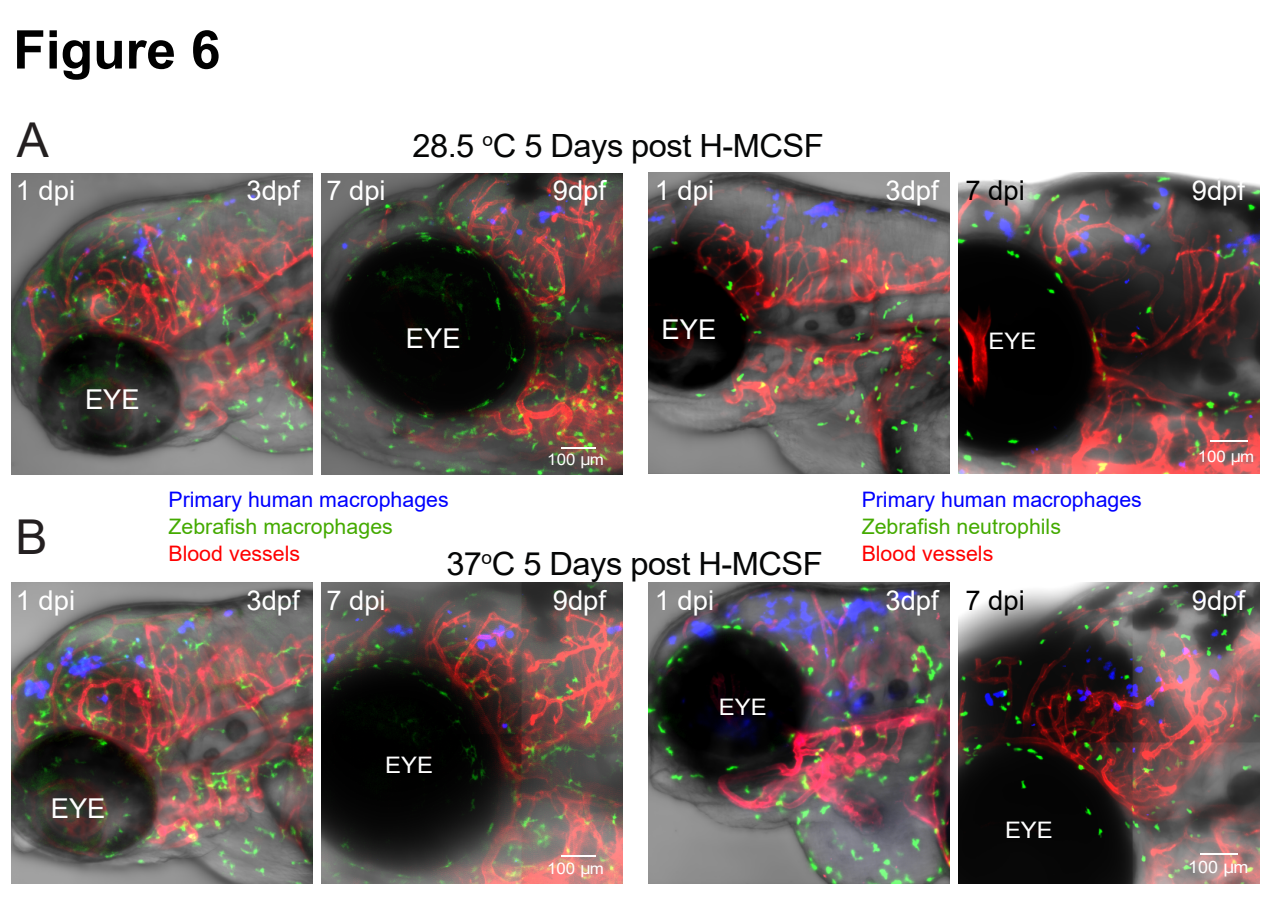
A
28.5 °C 5 Days post H-MCSF
1 dpi
3dpf
EYE
7 dpi
9dpf
EYE
100 µm
1 dpi
3dpf
EYE
7 dpi
9dpf
EYE
100 µm
Primary human macrophages
Zebrafish macrophages
Blood vessels
Primary human macrophages
Zebrafish neutrophils
Blood vessels
B
37°C 5 Days post H-MCSF
1 dpi
3dpf
EYE
7 dpi
9dpf
EYE
100 µm
1 dpi
3dpf
EYE
7 dpi
9dpf
EYE
100 µm

Figure 7

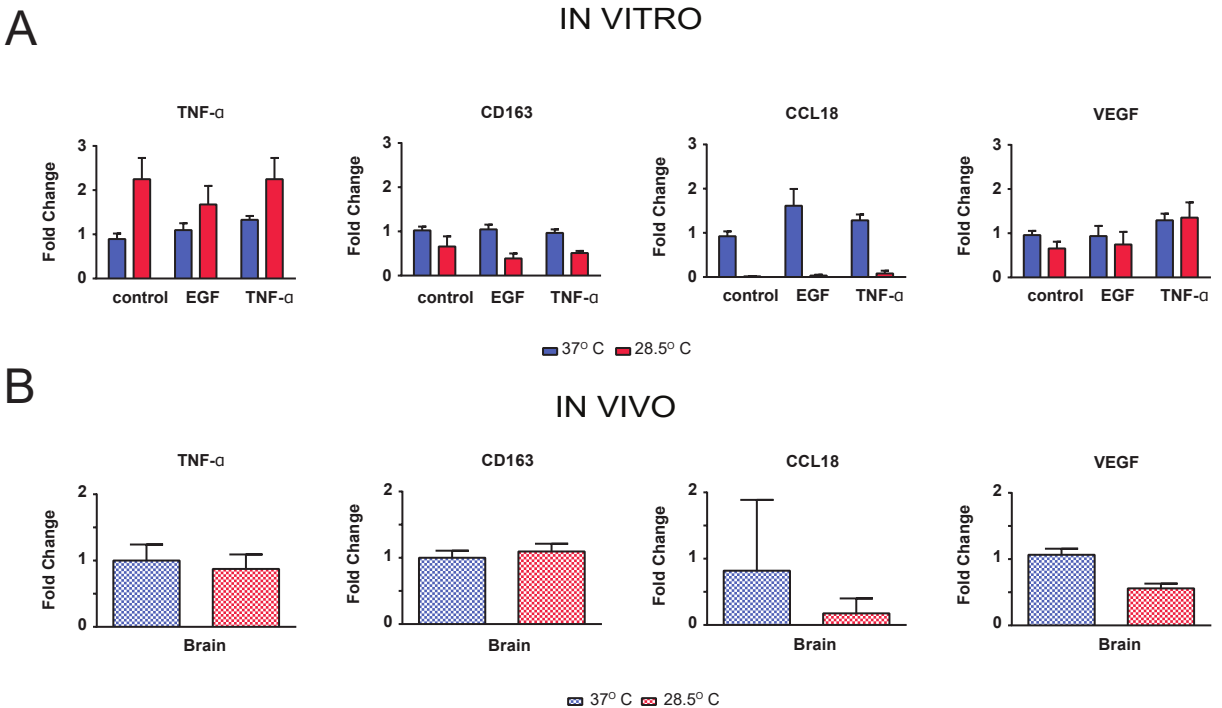
A
IN VITRO
TNF-α
CD163
CCL18
VEGF
Fold Change
0
1
2
3
control
EGF
TNF-α
37° C
28.5° C
B
IN VIVO
TNF-α
CD163
CCL18
VEGF
Fold Change
0
1
2
Brain
37° C
28.5° C

Supplementary Figure 1

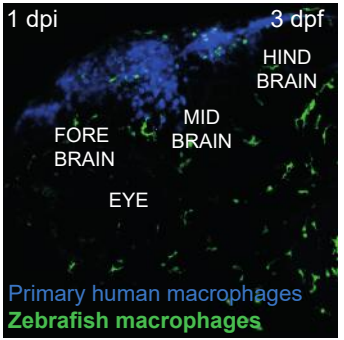

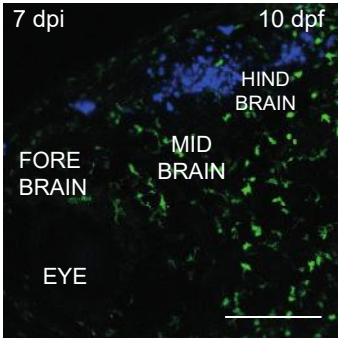

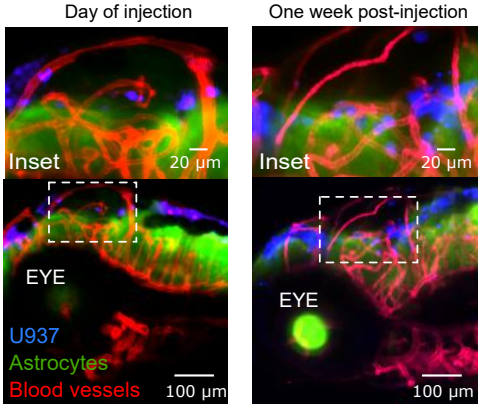

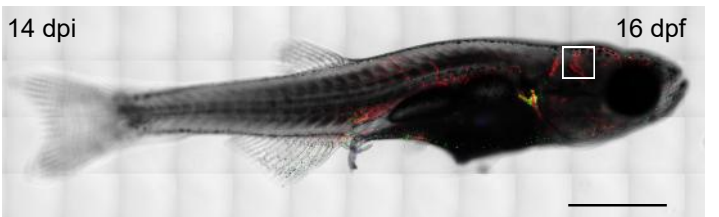

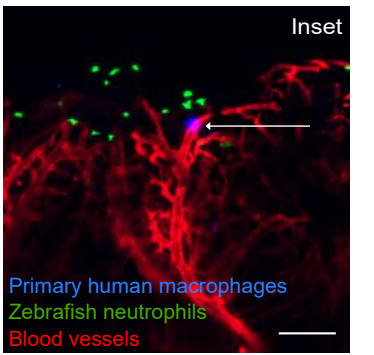

Supplementary Figure 2

A

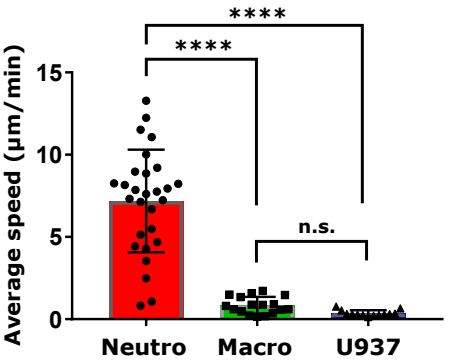

B

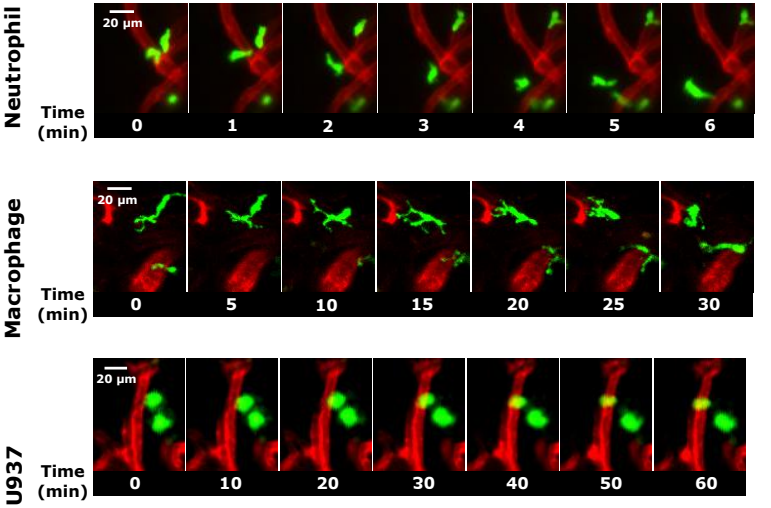

Supplementary Figure 3

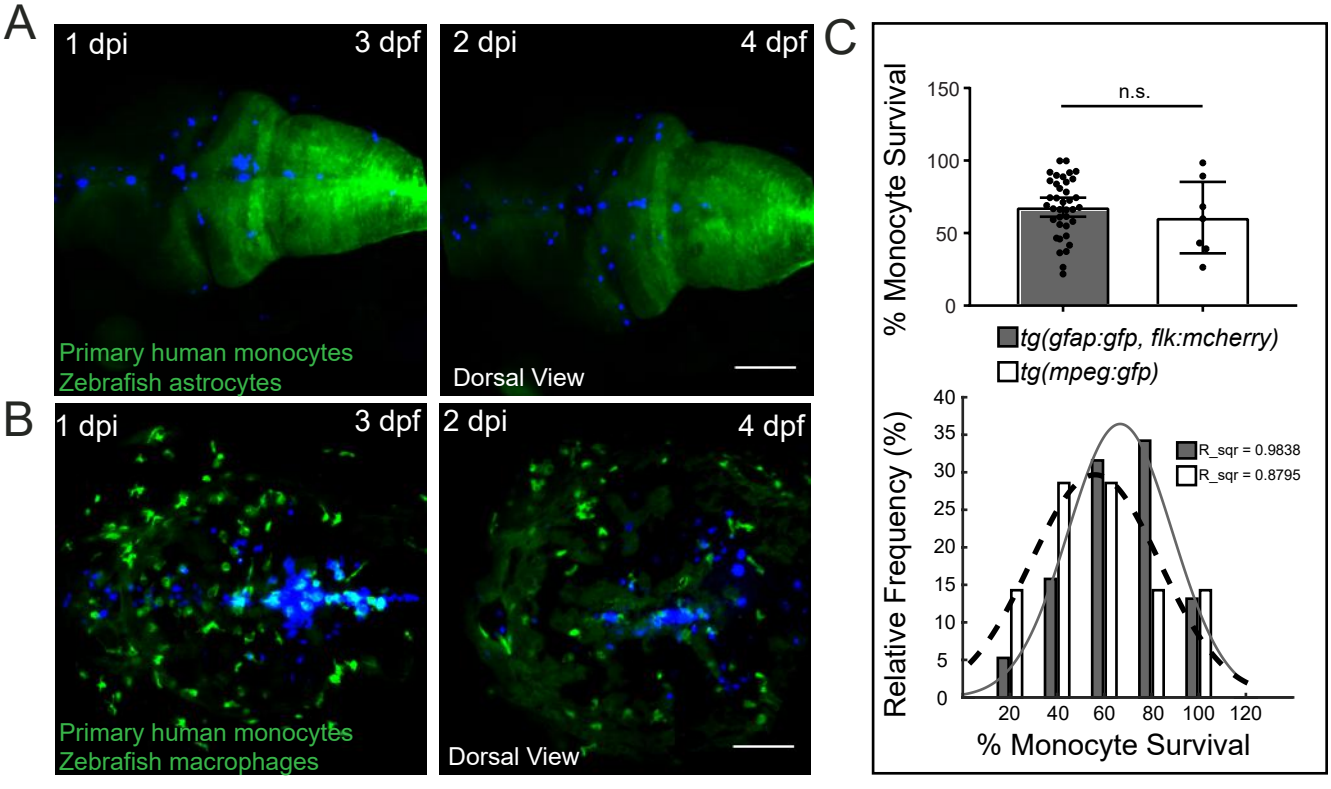

Supplementary Figure 4

A

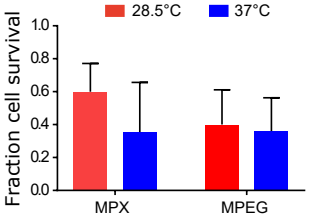

B

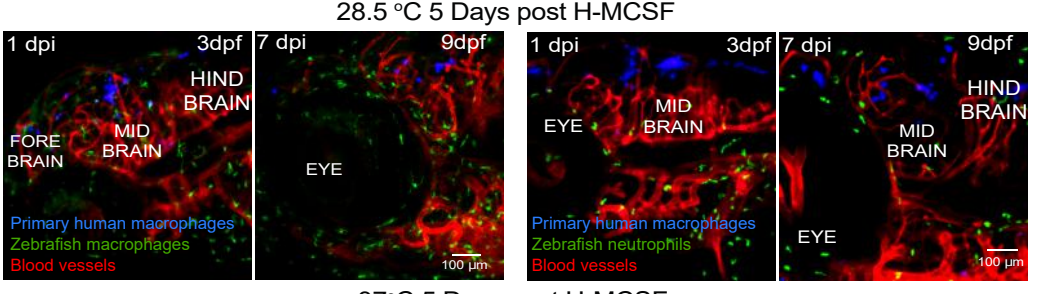

C